Department of Physics
University of Southern California
Los Angeles, California 90007

Semi-Annual Status Report

No. 7

for the

6 month period ending 31 August 1965

on

VACUUM ULTRAVIOLET RADIATION AND SOLID STATE PHYSICS

sponsored by the

National Aeronautics and
Space Administration

Grant No. NsG-178-61

submitted by

G. L. Weissler
Chief Investigator

15 October 1965

"VACUUM ULTRAVIOLET RADIATION AND SOLID STATE PHYSICS"

Department of Physics
University of Southern California
Los Angeles, California 90007

During the last half-year, progress has been made in three separate areas:

1) the optical constants, namely the index of refraction n and the extinction coefficient k, were obtained for 45 separate barium surfaces and 2 silver surfaces, all deposited and maintained in a vacuum of about 5×10^{-10} torr;

2) the grazing incidence monochromator has provided preliminary measurements of grating efficiencies down to 118 Å; and

3) optical constants of surfaces and thin films maintained in conventional vacua of 10^{-5} torr and measured at grazing incidence down to 100 Å.

The following will provide in somewhat greater detail the progress made in the above three areas.

1. Vacuum Ultraviolet Photon Interactions with Surfaces Maintained in an Ultrahigh Vacuum.

Since late November 1964 an ultrahigh vacuum of 3×10^{-10} torr has been achieved consistently in our stainless steel experimental chamber. The first results on measuring the reflectivity of barium surfaces deposited

and kept under conditions of ultrahigh vacua were obtained late in December 1964. These results and subsequent ones have been reported at the solid state physics meeting of the American Physical Society in Kansas City.[1] To remind the reader, the experimental arrangement is represented schematically in Fig. 1, where the ultrahigh vacuum chamber is shown on the right-hand side and the monochromator on the left. As is apparent in this figure, reflectivities from a sample surface can be determined at two angles, one near normal and the other near grazing incidence. Light from the monochromator passes into the ultrahigh vacuum chamber through sapphire windows. This fixes the short wavelength limit of transmission to somewhere near 1500 Å. The reflectance values so obtained for two angles of incidence as a function of wavelength permit the calculation[2] of the complex dielectric constant, ε, and subsequently the imaginary portion $(1/\varepsilon)$. This $\mathrm{Im}(1/\varepsilon)$ is proportional to the characteristic energy losses which electrons suffer when passing through a thin film. Such experiments have been done by a variety of groups.[3] Thus, it is possible to make a comparison between the two. Such a comparison is presented

---

[1] E. I. Fisher, I. Fujita, and G. L. Weissler, Bull. Am. Phys. Soc. 10, 375 (1965).

[2] R. Tousey, J. Opt. Soc. Am. 29, 235 (1939); I. Simon, ibid. 41, 336 (1951); K. Ishiguro, T. Sasaki, and S. Nomura, Scientific Papers of the College of General Education, Univ. of Tokyo 10, 207 (1960); ibid. 12, 19 (1962).

[3] J. L. Robins and P. E. Best, Proc. Phys. Soc. (London) 79, 110 (1962).

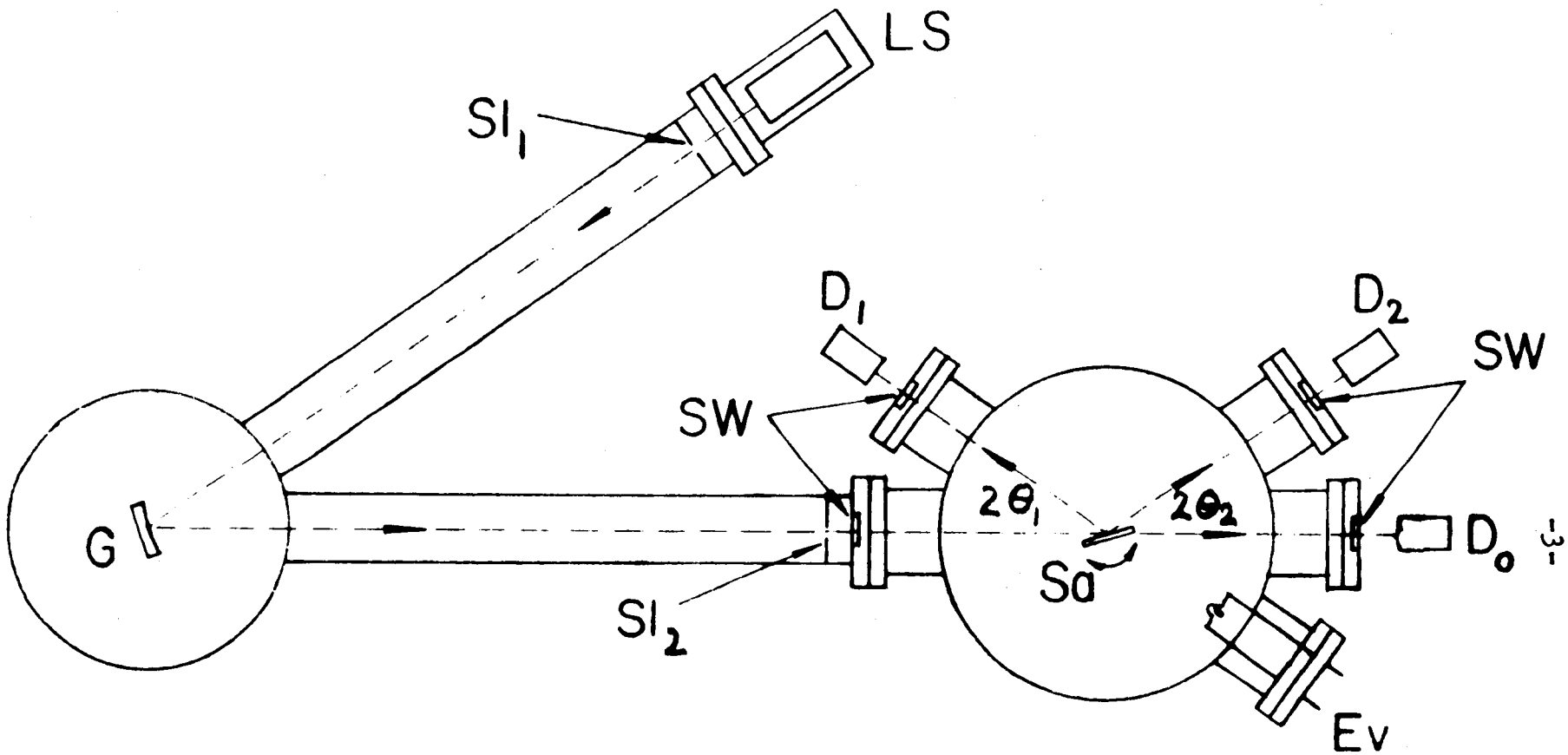

Fig. 1 Ultra-High Vacuum Reflectivity Chamber with Sapphire Windows (SW). The external vacuum monochromator is shown to the left of the chamber. Radiation from a light source (LS) passes through the entrance slit (Sl_1) and illuminates the grating (G) which disperses it. Consequently, monochromatic light emerges from the exit slit (Sl_2), passes through a sapphire window into the ultra-high vacuum chamber where the sample (Sa) reflects at a near normal incidence angle θ_1 to the detector (D_1) or at a near grazing incidence angle θ_2 to the detector (D_2). The incident intensity may be measured with the sample removed by using the detector (D_0). The sample may be evaporated onto its holder using the filament (Ev).

in Fig. 2, where the imaginary portion (1/s), as obtained from our reflectance measurements, is plotted as the ordinate and the wavelength at which these reflectance measurements were made as the abscissa in units of electron volts (eV). The experimental results obtained from measuring characteristic electron energy losses[3] is represented by a vertical downward arrow in this figure. The coincidence between the peak of our optical data and the results from characteristic electron losses is very gratifying. Further work on barium has been concerned with variations of techniques. For example, different substrata have been tried onto which the film was evaporated. At the time of this writing it is clear that the reproducibility of our optical data is such as to allow us to go on soon to other materials.

The planning of proposed future research in the area of ultrahigh vacuum reflectivities must take into account the fact that the USC Physics Department and therefore our vacuum ultraviolet group will be moving into a new building by the end of 1965 or the beginning of 1966. Because of this move, it is essential to adapt our plans to this move in order to avoid unnecessary duplication of assembly of apparatus.

For this reason it is proposed to use the present ultrahigh vacuum chamber, which is limited optically down to 1500 Å by sapphire windows, in the same mode as it has been used on the barium surfaces (see Fig. 1). The new surfaces to be investigated in the next half-year with the present experimental arrangement will be silver, which promises

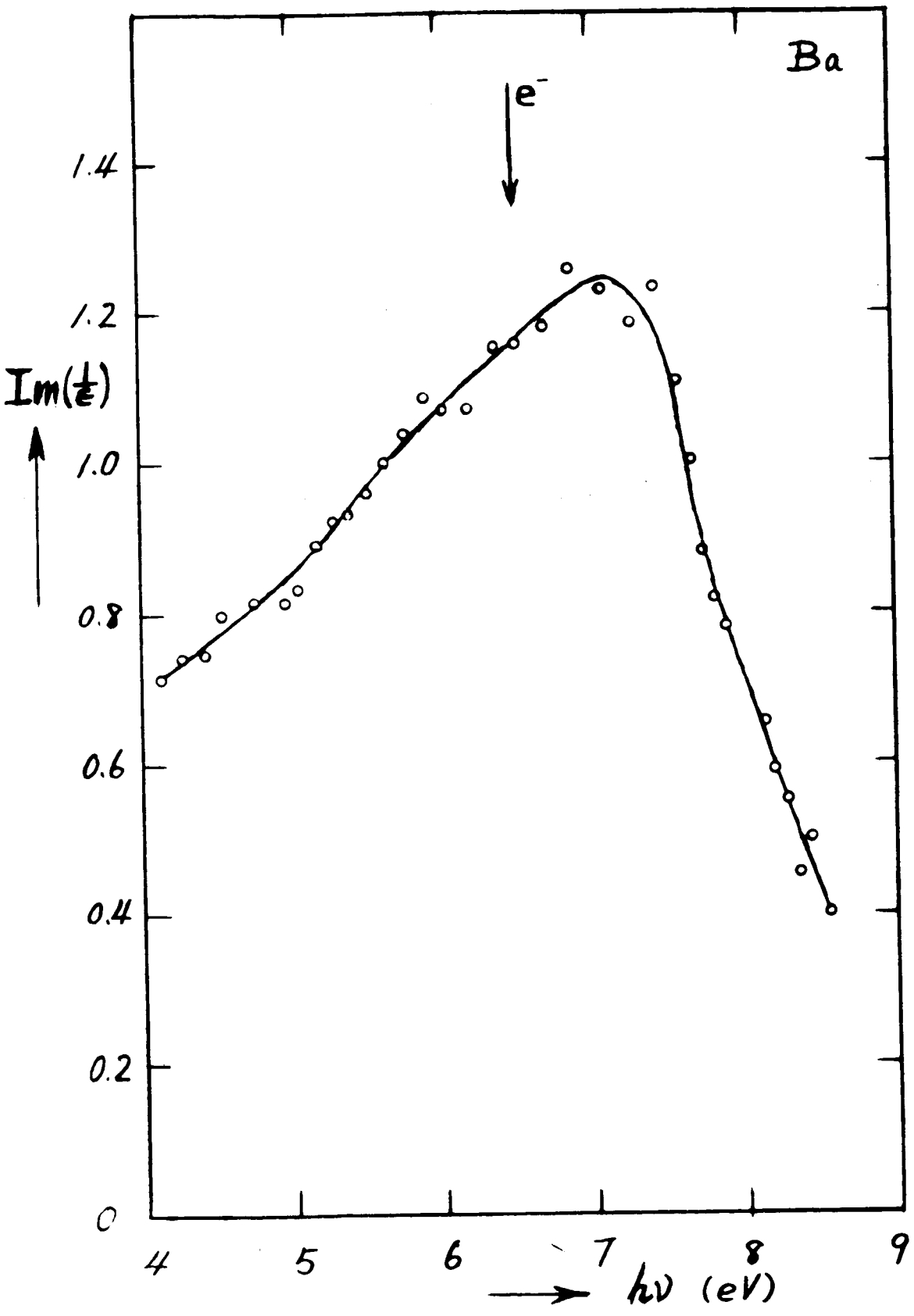

Fig. 2. Reflectance data of Ba converted (see ref. 2) to the imaginary part of the dielectric constant, ε, plotted against photon energy. The maximum of this curve may be compared to the characteristic electron energy loss value, shown by the downward pointing arrow marked e^- and obtained in an independent experiment by Robins and Best.[3]

interesting results near 3100 Å where older reflectivity data have shown a pronounced dip. After silver, it is proposed to look at the alkalis, particularly lithium (characteristic electron energy loss about 8 eV), sodium (6 eV), potassium (4 eV), and perhaps rubidium (4 eV) and cesium (3.5 eV). These alkali metals are much more reactive than barium and may not remain uncontaminated for a sufficiently long time to make the required optical reflectance measurements. However, our present experience with barium offers grounds for optimism, since it shows recognizable contamination only after several days of exposure to a vacuum of the order of 10^{-10} torr. Taking into account the higher reactivity of the alkali metals, we feel that within at least the first hour after deposit the reflectance measurements should be representative of an uncontaminated alkali surface.

It is anticipated that measurements in the present chamber of silver surfaces and of one or more alkali surfaces will keep this particular program active in a productive manner until the apparatus needs to be transferred to our new quarters.

Simultaneously with the continuation of reflectance measurements in the system shown in Fig. 1, an effort is presently underway in terms of testing and gaining experience with a second ultrahigh vacuum system as presented in Fig. 3. This system differs from the existing ultrahigh vacuum chamber: there will be no oils used anywhere in the pumping lines; commercial sorption pumps are used to reduce

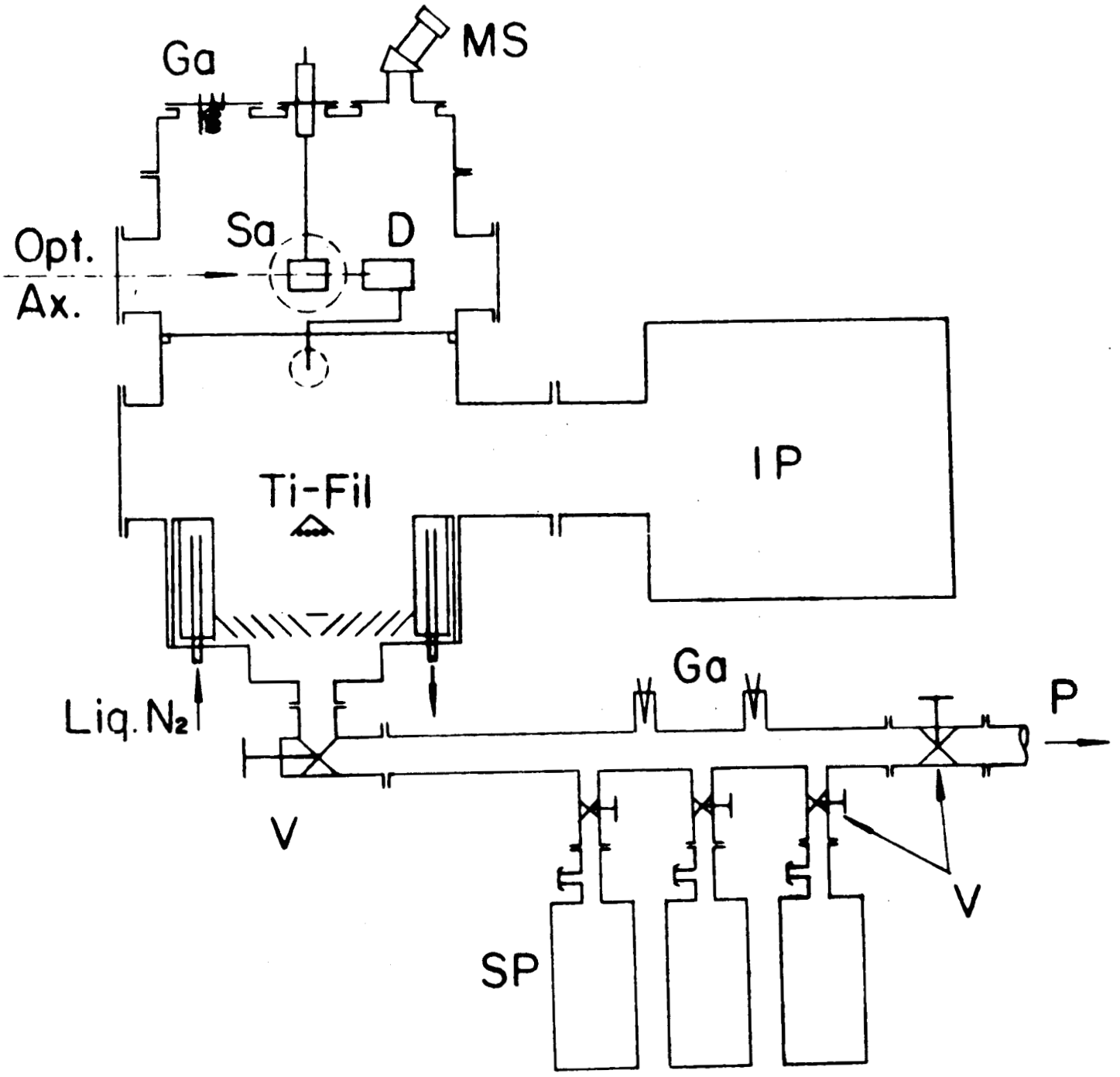

Fig. 3 New Ultra-High Vacuum Reflectivity Chamber with Internally Mounted Light Detectors (D). An ion gauge (Ga) and a mass spectrometer (MS) monitor the environment of the sample (SA), maintained by an ion pump (IP) and by sublimation of titanium (Ti-Fil) which is deposited on surfaces cooled by liquid nitrogen (Liq. N_2). The fore vacuum is provided by chemical sorption pumps (SP), which can be valved off (V). With the exception of the fore-vacuum line, the entire system can be baked at 400°C.

the pressure from atmospheric values down into the micron range, and an ion pump together with a titanium evaporator will allow a further reduction down into the 10^{-10} torr range. This system is presently undergoing helium leak detector testing. It is anticipated that an ultrahigh vacuum can be achieved in this new chamber also by the end of 1965, perhaps sooner. New devices will be tested in this separate chamber; for instance, it has become abundantly clear that the region of the evaporating filament needs to be differentially pumped during the time of evaporation of the target film. Some relatively simple schemes to achieve this have been sketched out and will hopefully be tried during the next half-year. This will allow the dposition of thin films without having them absorb simultaneously those gases or impurities which are unavoidably liberated during evaporation.

After the present equipment has been transferred into the new building, it is planned to reassemble early in 1966 the present ultrahigh vacuum chamber with sapphire windows (see Fig. 1) and the new ultrahigh vacuum chamber presently under test (see Fig. 3). These two ultrahigh vacuum systems will then be combined as showin in Fig. 4: there, the old ultrahigh vacuum system (Fig. 1) is shown on the left as the grating chamber of a Seya monochromator which can be held at or near ultrahigh vacuum pressures, of the order of 10^{-9} torr. The exit slit of this Seya monochromator allows monochromatic light to enter into the new ultrahigh vacuum chamber (Fig. 3). This light will pass through the exit slit <u>without</u> having to

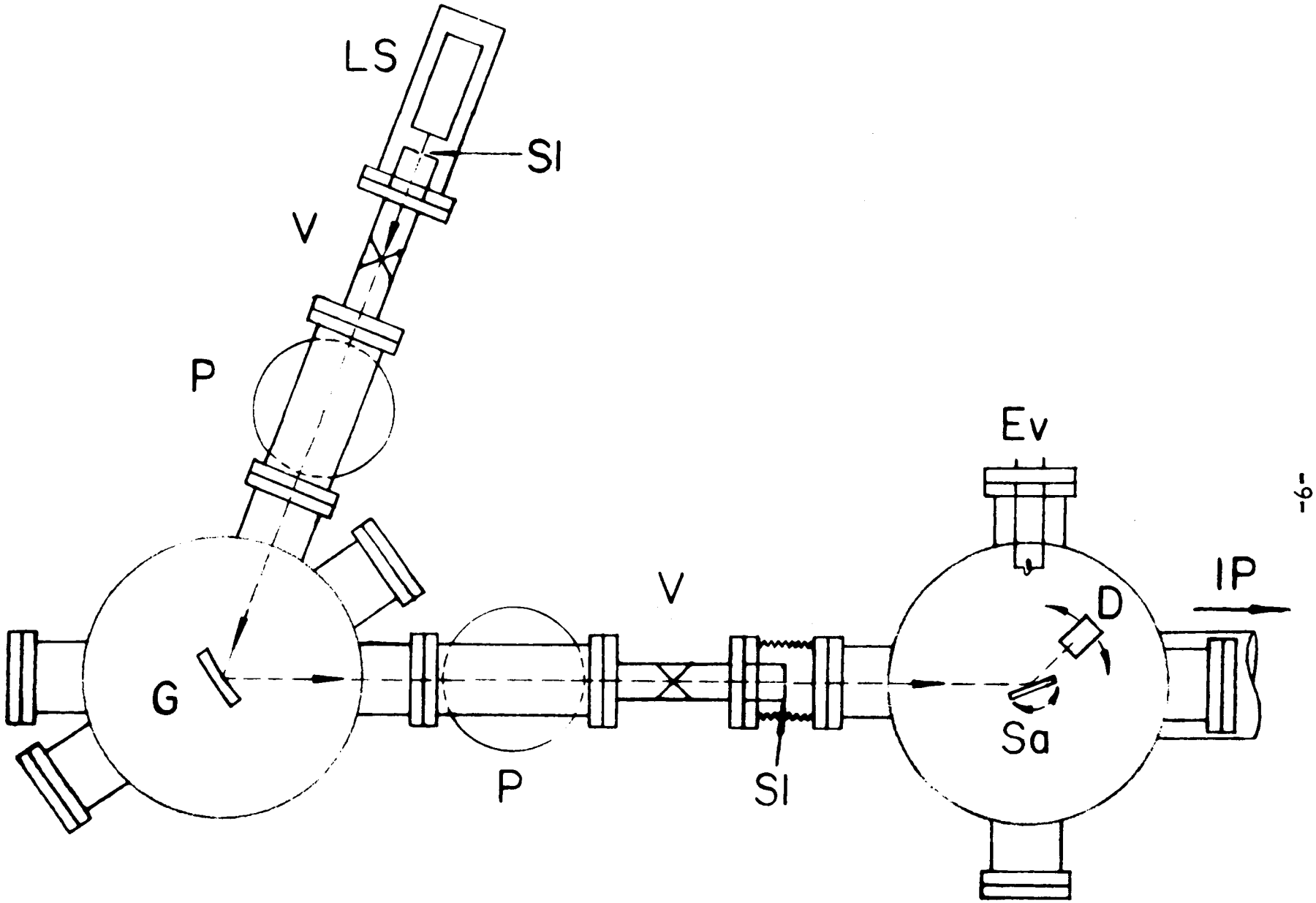

Fig. 4 New Ultra-High Vacuum Reflectivity Chamber Combined with Seya Monochromator also Operated in an Ultra-High Vacuum Using Chamber of Fig. 1. Nomenclature and procedure used in Fig. 1 apply here, except the monochromatic beam passes through slits without use of windows into the new reflectivity chamber, and an internal light detector (D) is used there.

traverse any optical window material. Thus, the wavelength range of this combination will be from 10,000 Å down to 250 Å, the lower limit of the Seya mounting. This extension of our present work to the shorter wavelength below 1000 Å will make it possible to investigate the optical properties and particularly the reflectance of such thin films as Al, Te, Bi, Pb, Ge, Si, and many others. These particular films all have in common characteristic electron energy losses or plasma frequencies of the order of 10 eV or greater (below 1200 Å). It is hoped that a similar comparison can be made for a wide variety of these materials with the optically determined imaginary part of $(1/\varepsilon)$ and the experiments on electron characteristic energy losses by other groups.

In addition, photoelectric yields from clean surfaces kept under ultrahigh vacuum conditions will be measured in this apparatus. Our present knowledge on photoelectric yields is limited to surfaces maintained in vacua not much better than 10^{-8} torr. The undersigned is not aware of any absolute yield measurements of electrons released per photon absorbed from films produced and maintained at vacua of 10^{-10} torr and in the vacuum ultraviolet region.

2. Grazing Efficiencies down to 118 Å.

During the first part of this year until 15 June 1965, a set of measurements was conducted on seven gratings in order to determine grating efficiencies between 150 Å and 923 Å and for a number of angles of incidence ranging from near normal to the Seya angle, 35°, to near grazing incidence. In

addition, each of these seven gratings has been subjected to electron microscopic measurements with the help of Professor R. Baker of the USC Medical School, and micrographs are available with magnifications up to 50,000 for 5 blazed gratings* and 2 unblazed lightly ruled glass gratings‡ (Siegbahn-type gratings).

The optical efficiency work and the electron microscopy is finished, and at the present time, the material is being prepared for another Master's thesis and for a technical report which should be available within two months.

It may be worthwhile to summarize some of these grating efficiency measurements. If the grating efficiency is defined arbitrarily for any given monochromatic radiation as the ratio of the intensity of the diffracted light, I_1, for a given order (first or second order, inside or outside) to the intensity of the incident light, I_o, then this particular fraction I_1/I_o increases from 0 angle of incidence (normal) to a near grazing angle (60 to 80°) and then declines toward still greater angles of incidence (approaching 90°). The observed intensity maximum occurs at that angle for which the fixed blaze angle of the grating would predict a theoretical maximum. When the intensity ratio I_1/I_o is plotted against wavelength for a fixed angle of incidence, then again the

---

*Courtesy of Mr. David Richardson, Bausch and Lomb, Inc., Rochester, New York.

‡Manufactured by G. Gomez, 538 Franklin Place, Monrovia, California.

maximum occurs at a wavelength for which the theory predicts such a maximum for a fixed blaze angle. Examples of such measurements are shown in Figs. 5, 6, 7, and 8, which are for the most part self-explanatory. A very interesting part of these experiments is the fact that a blazed replica grating from Bausch and Lomb coated with either gold or platinum is substantially more efficient, by a factor of 2 to 10, than a lightly ruled glass grating (Siegbahn-type) or an aluminum-coated grating, if used in the short wavelength region at near grazing angles of incidence.

In addition to these general results, the electron microscopy affords a good comparison between the surfaces of these gratings. For instance, the undisturbed glass surface of the Siegbahn-type grating is not materially smoother than the grooved surface of a Bausch and Lomb replica grating, blazed at 1°. In addition, the electron micrographs show that some of the Bausch and Lomb gratings have considerable amounts of undistrubed or non-ruled area between rulings. They, therefore, act as a combination of Siegbahn-type and blazed-type gratings.

Even before the evaluation of these existing experimental data has been completed, it seems obvious that blazed gratings with gold coatings are to be preferred over Siegbahn-type gratings if the wavelength range under investigation lies between 50 Å and 500 Å.

After the grating efficiencies have been submitted as a technical report the material will be presented in somewhat condensed form for publication in one of the scientific journals.

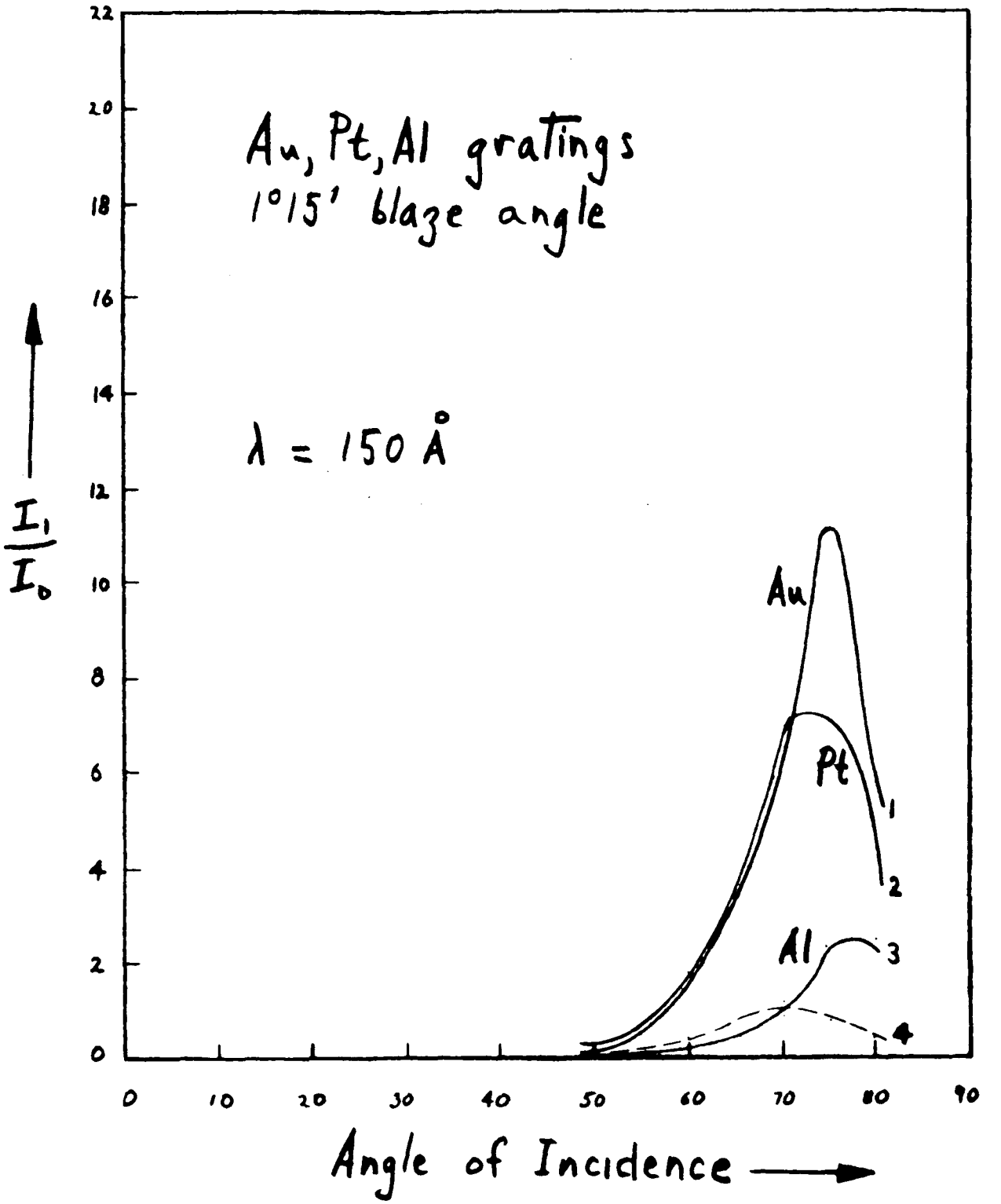

Fig. 5. The grating efficiency of Bausch and Lomb blazed gratings at 150 Å, as a function of angle of incidence. The curves show the experimentally determined ratio I_1/I_0, of the first order diffraction intensity to incident intensity of the monochromatic radiation. The solid curves are measurements on the blazed side. The broken curve represents the I_1/I_0 ratio for the gold and platinum gratings on the unblazed side; the corresponding curve for aluminum lies about half way between this curve and the abscissa. All the gratings were replicas of 1 meter radius and 600 lines per millimeter, blazed for 580 Å at normal incidence.

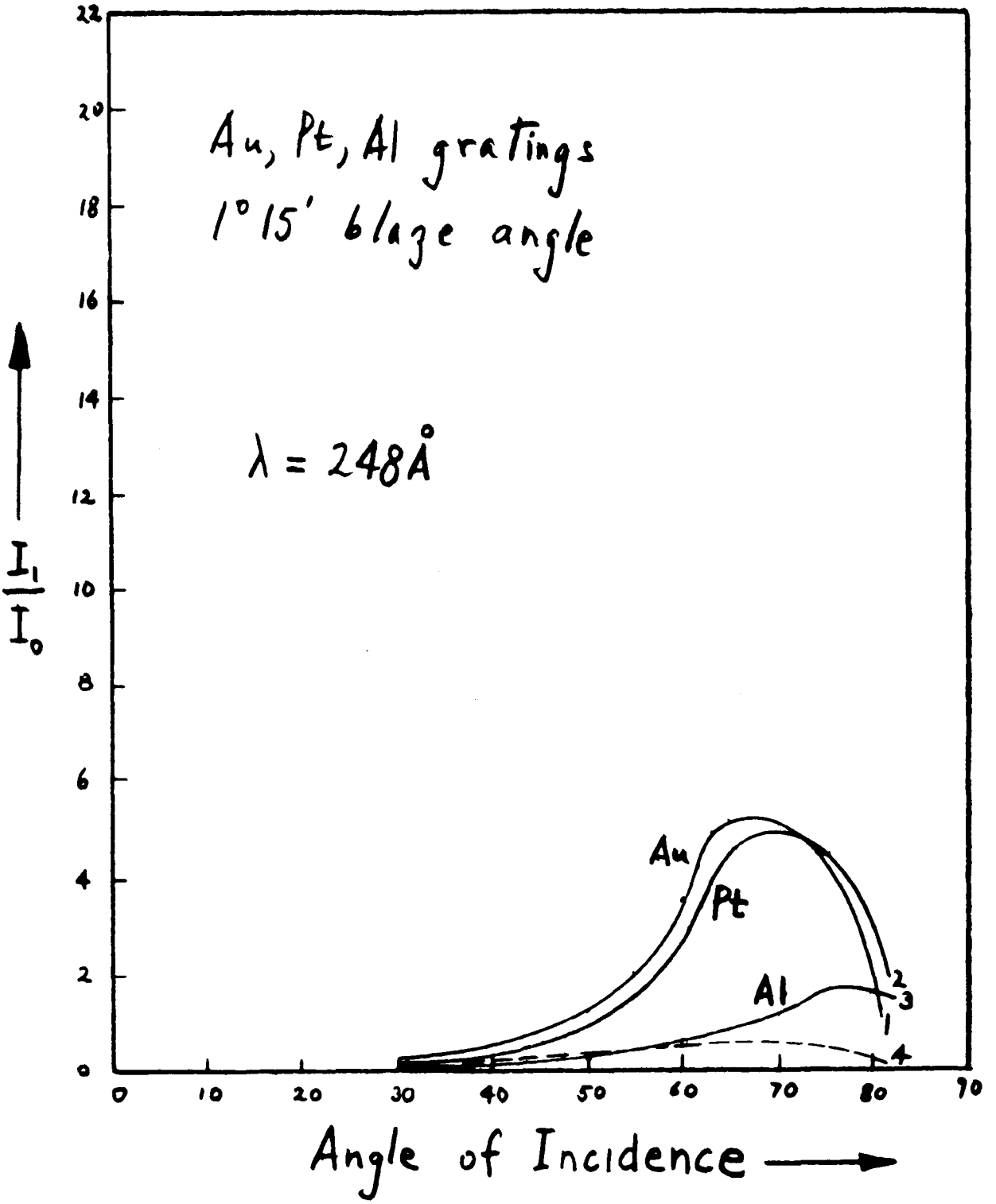

Fig. 6. The grating efficiency of Bausch and Lomb blazed gratings at 248 Å, as a function of angle of incidence. The curves show the experimentally determined ratio I_1/I_0 of the first order diffraction intensity to incident intensity of monochromatic radiation. The solid curves are measurements on the blazed side. The broken curve gives the I_1/I_0 ratio for the gold and platinum gratings, on the unblazed side; the corresponding curve for aluminum lies somewhat lower. All the gratings were replicas of 1 meter radius of curvature and 600 lines per millimeter, blazed for 580 Å at normal incidence.

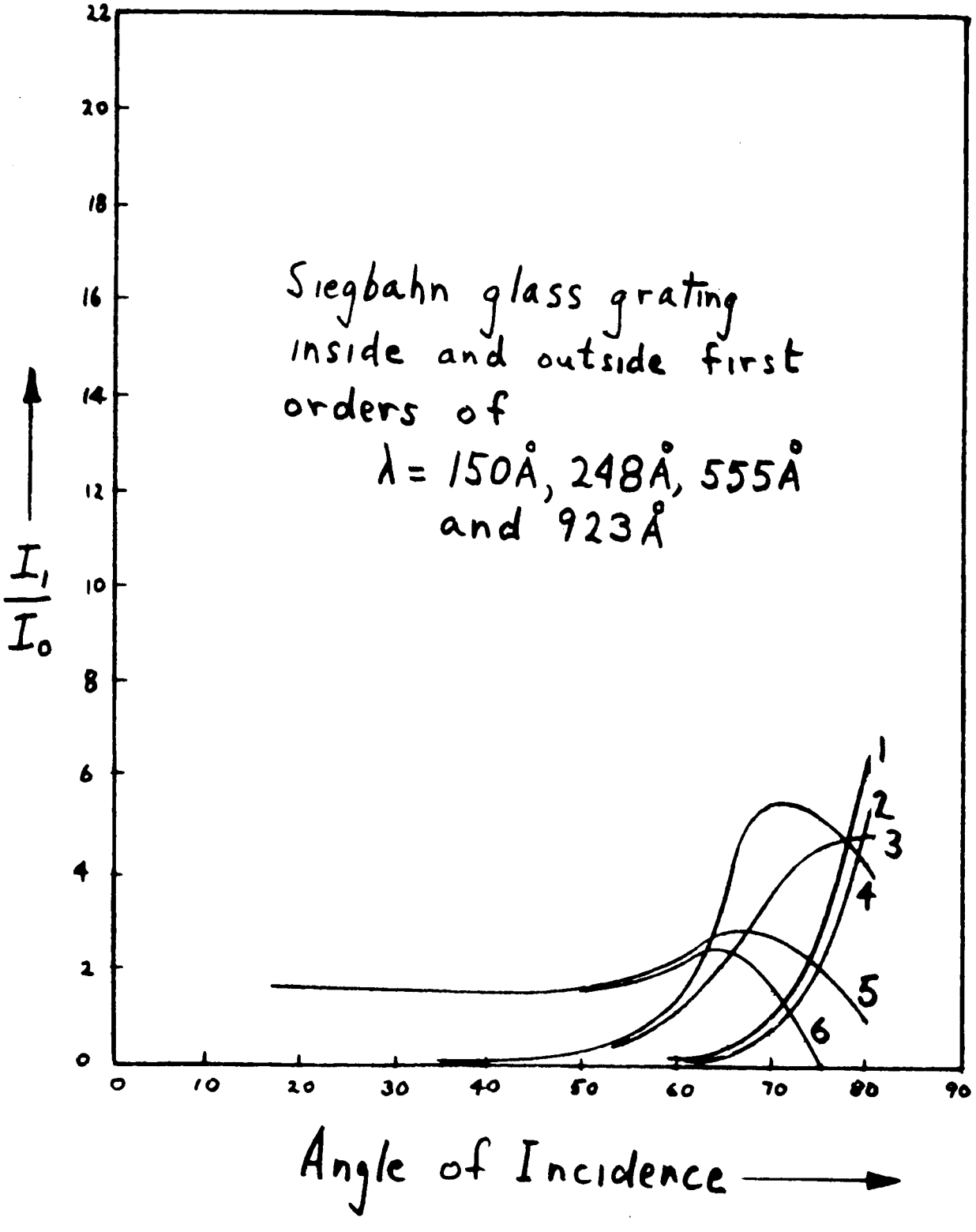

Fig. 7. The grating efficiency of a lightly ruled (Siegbahn) grating, ruled on glass, as a function of angle of incidence. The curves show the experimentally determined ratio I_1/I_0 of first order intensity to incident monochromatic radiation intensity. Curve 1 is the first inside order, and curve 2 the first outside order of the 150 Å radiation. Curve 3 is the first inside order, and curve 4 the first outside order at 248 Å. Curve 5 is the first inside order, and curve 6 the first outside order at 555 Å. The grating had a radius of curvature of 1 meter, and had 600 lines per mm.

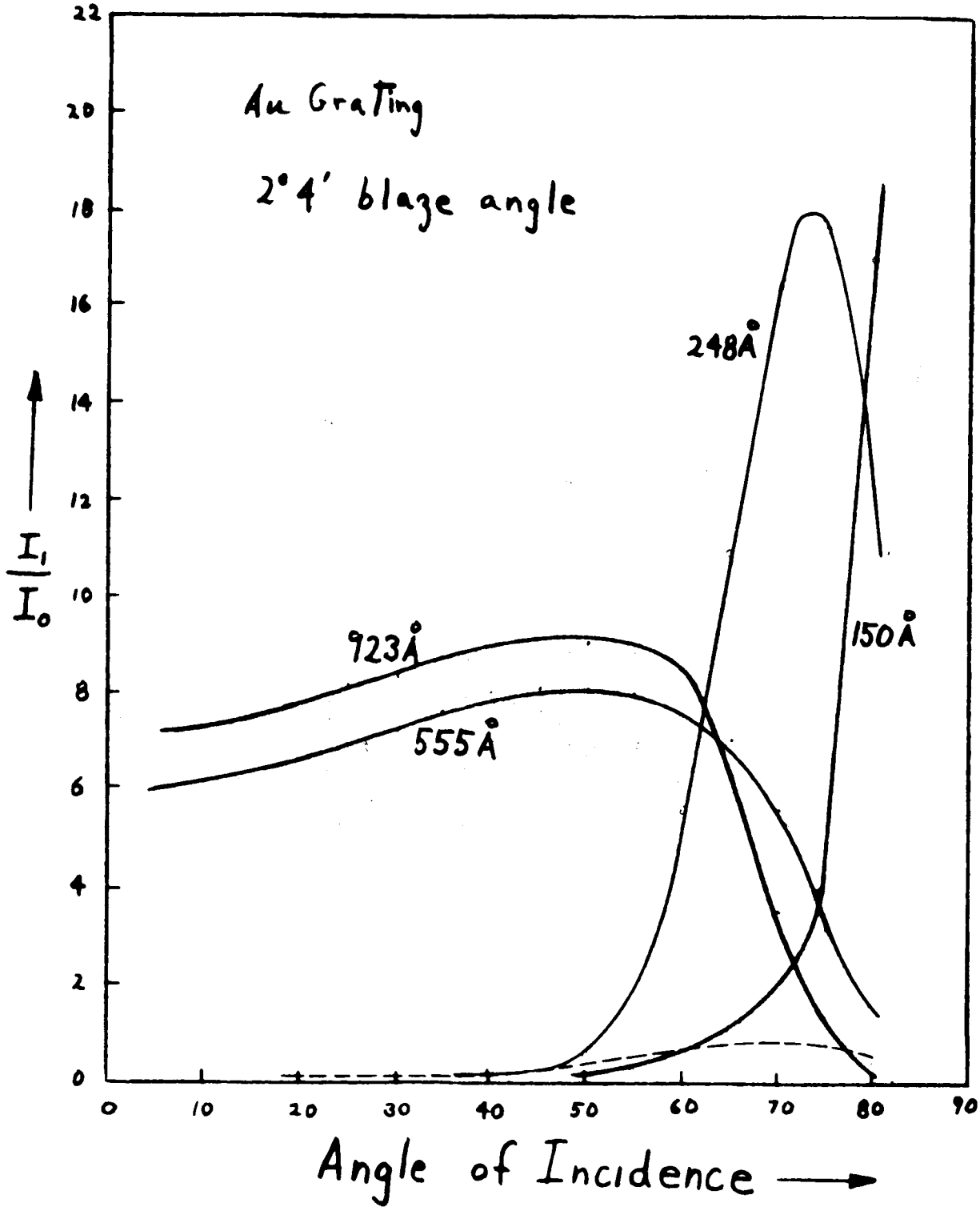

Fig. 8. The grating efficiency of a Bausch and Lomb gold coated grating, blazed for 1210 Å, as a function of angle of incidence. The curves represent the ratio I_1/I_0 of the first order intensity to the incident monochromatic intensity. The solid curves are measurements on the blazed side. The broken curve represents this ratio on the unblazed side. The grating was a replica of 1 meter radius of curvature and 600 lines per millimeter. The manufacturer quoted a blaze wavelength of 1210 Å, at normal incidence.

3. Optical Constants of Surfaces and Thin Films Maintained in Conventional Vacua of 10^{-5} torr and Measured at Grazing Incidence down to 100 Å.

Fig. 9 indicates the experimental arrangement in which a Vodar grazing incidence monochromator is coupled to a large, 18" diameter experimental chamber. The Vodar instrument allows the exit slit to remain focused when scanning the spectrum, i.e., the entrance slit (together with the light source) and the grating are moved by a scanning mechanism in such a fashion that at all wavelengths they lie on a proper Rowland focusing circle. Between the exit slit of the monochromator and the 18" diameter experimental chamber there is placed an intermediate chamber which allows a totally absorbing ion chamber (filled with a rare gas) to be moved into the light beam. The total number of ion pairs per second produced in this chamber by the mechanism of photoionization is exactly equal to the total number of photons absorbed. This allows absolute photon flux measurements to be made in conjunction with a variety of experiments to be undertaken in the 18" experimental chamber. Preliminary results are shown in Table I. In the past year, reflectivities of p- and n-doped silicon crystals have been measured. The results have led to a Master's thesis and a technical report.[4]

Some advances in vacuum ultraviolet instrumentation, particularly on light source development and on the use of

---

[4] J. Earl Rudisill, Tech. Rep. No. USC-VacUV-100, dated 7 May 1965, Contract NsG-178-61.

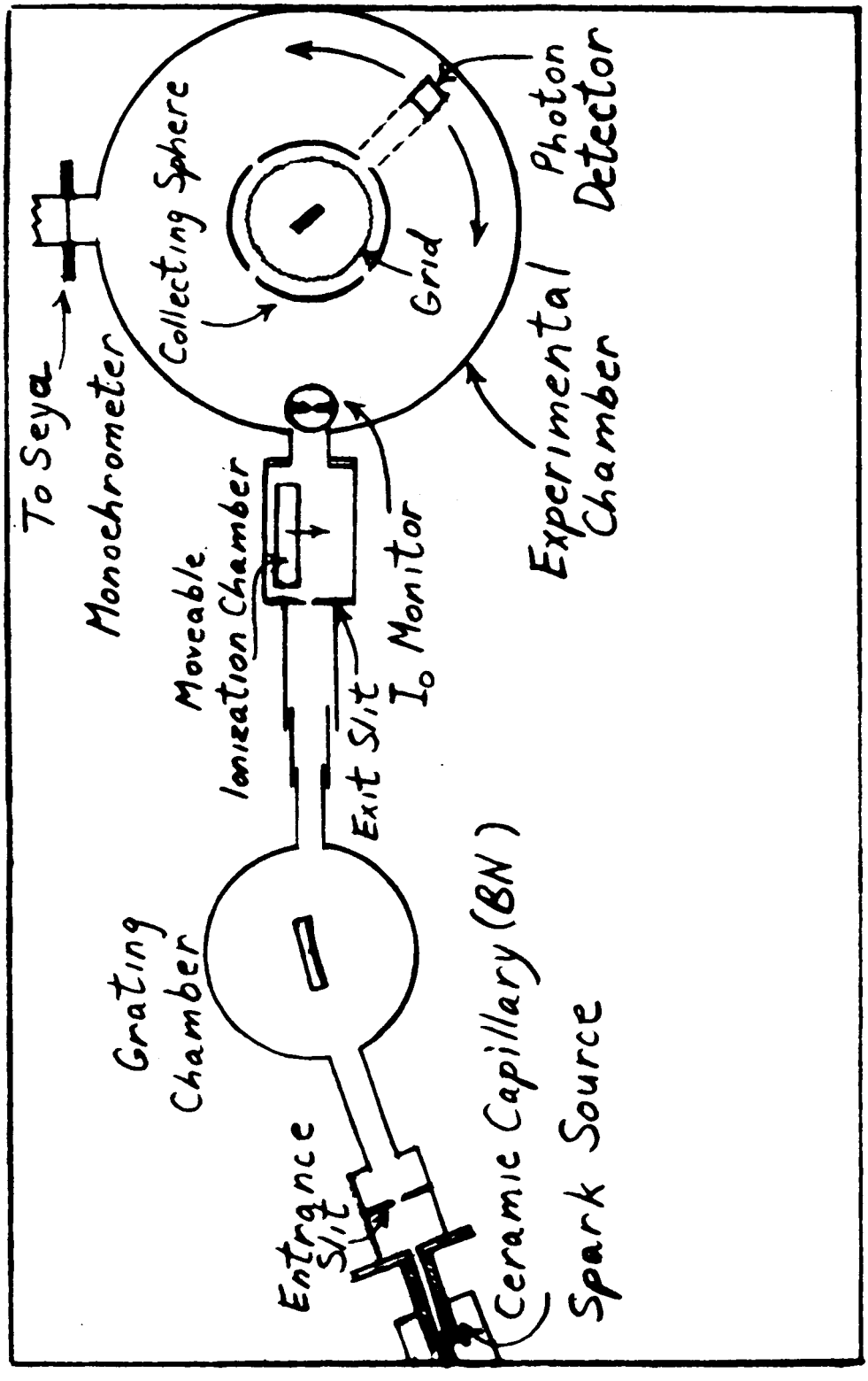

Fig. 9. Vodar grazing incidence monochromator and the 18" diameter experimental chamber. An ionization chamber is positioned behind the exit slit to measure the incident photon flux.

TABLE I

Currents from total absorption Argon flow ionization chamber for various incident photon wavelengths.
Collecting voltage was $22\frac{1}{2}$ V.
10^{-11} amps = 6.25×10^{7} electrons/second or photons/second.

λ (Å)	I (amps)
248	0.95×10^{-11}
260	0.15
266	0.5
288	0.35
303	0.45
323	0.35
374	0.3
459	0.25
508	0.35
555	1.1
625	0.6
702	0.5
760	1.1

a pre-disperser down to 100 Å, have been reported as an invited paper[5] at the International Commission of Optics Conference in Tokyo and Kyoto, Sept. 2 to 8, 1964.

Since the completion of this work on grating efficiencies in June 1965, the electrode system for the main purpose of this apparatus was installed in the 18" diameter experimental chamber. This electrode system consists essentially of a thin film target holder, which can be moved up and down (into or out of the optic axis) and rotated about its vertical axis in order to change the angle of incidence of the monochromatic light from the Vodar monochromator. Fig. 10 shows at its center the thin film target holder. Arranged around the target holder as its center is a spherically shaped screen and behind the screen a solid copper sphere cut up into octants. The purpose of this electrode configuration is to measure the following quantities:

1. Incident monochromatic light flux in units of photons per second.

2. Reflected intensity, by rotating a photomultiplier about the target in a horizontal plane. This photomultiplier moves outside the spherical electrodes and receives reflected light from the thin film sample which passes through the horizontal slot indicated in the equatorial plane of Fig. 10. This multiplier can measure relative light intensity: With the sample out of the way, I_o is measured; with the sample in

---

[5] G. L. Weissler, Japan. J. Appl. Optics, to be published (1965).

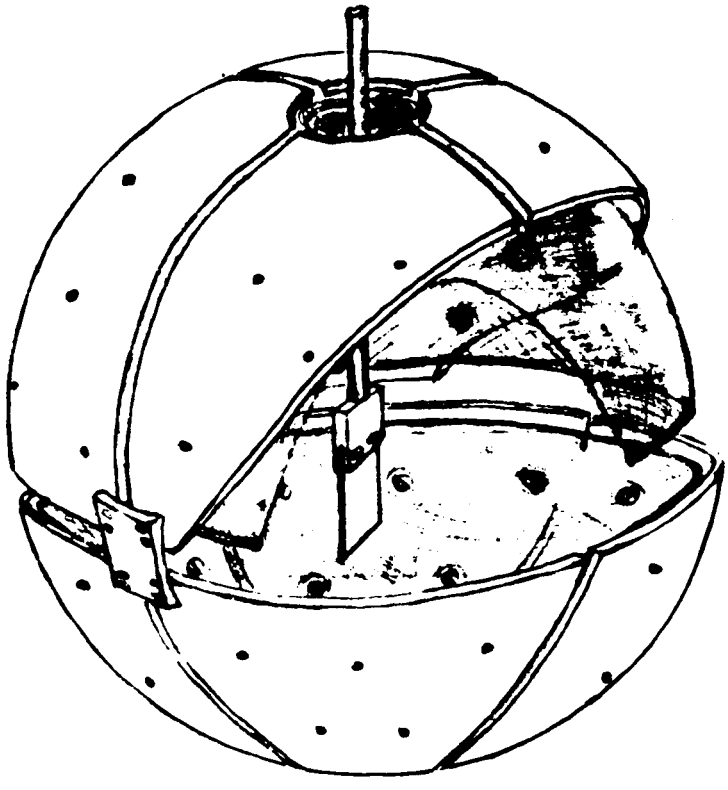

Fig. 10. Cut-away drawing showing the construction and geometry of the spherical collecting and retarding system.

the optical path, the transmittance can be measured; finally, by rotating the multiplier to the appropriate angle, the reflected intensity can be obtained. This allows the determination of the number of photons absorbed in a thin film.

3. The spherical electrodes are connected to low current feedthrough leads and allow the measurements of the total number of electrons emitted from the surface of this thin film sample or target. This can then be translated into photoelectric yield in units of photoelectrons emitted per photon absorbed.

4. By placing various counter potentials on the spherically shaped screen (which is located between the thin film sample and the solid spherical copper electrodes), it is possible to determine electron energy distributions.

5. By measuring both the photoelectric current as well as the distribution of energies of photoelectrons to selected octants of the solid copper sphere, one can determine whether more or less electrons are emitted in the forward direction than in the backward direction (where forward means in the direction of the light beam and backward against the direction of the light beam). In addition, it is possible to determine whether the electron energy distributions are different for those photoelectrons which are emitted nearly tangential to the thin film (thereby traveling through a greater thickness of material with correspondingly increased probability of electron-electron scattering) in contrast to those other photoelectrons which are emitted more nearly in a normal direction. Some preliminary results of this work have been obtained.

While the primary purpose of these early data is to test the operation of all measuring instruments, the information is nevertheless indicative of the great promise held out by more accurate measurements to be attempted in the near future.

Figure 11 shows a relative photoelectric yield as a function of the angle of incidence for a Au surface. All these curves are normalized to the same ordinate at the position of their maximum. It is interesting to see that the maximum yield in all cases occurs at rather large angles of incidence.

Figures 12 and 13 show the retarding potential versus electron current measurements which by differentiation have been translated into electron energy distributions in Figs. 14 and 15. While the interpretation at this particular time is premature, it is most certainly highly interesting that two distinct groups of energies are represented in this distribution, namely a large number of very low energy electrons and a small but distinctly measurable number of high energy electrons.

Figure 16 shows the relationship of the octants with respect to the target and the incident photon beam and helps to clarify the curves presented in Fig. 17, which represents the photoelectron currents collected by the various octants. The significance of these data is that a larger yield is recorded for the octant which collects electrons emitted more in the tangential direction from the surface. This indicates the importance of polarization of the light. One might expect that electrons in the metal, after having absorbed the energy of the incident photon, will be scattered a number of times

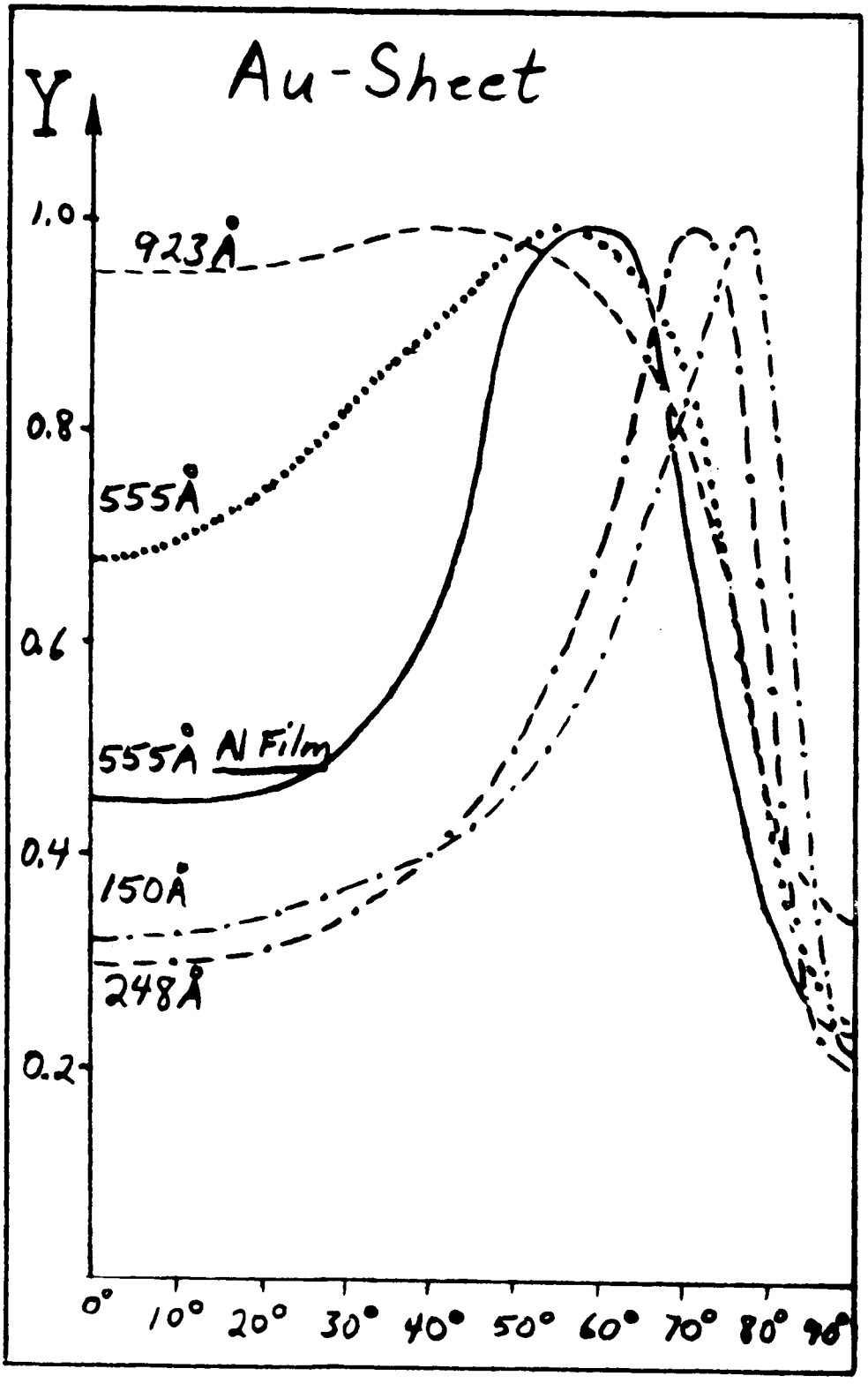

Fig. 11. Photoelectric yield, Y, of a 10 mil gold sheet as a function of the angle of incidence for various incident wavelengths. Curves are normalized to the value at maximum yield. Included for comparison is the yield of an evaporated aluminum film.

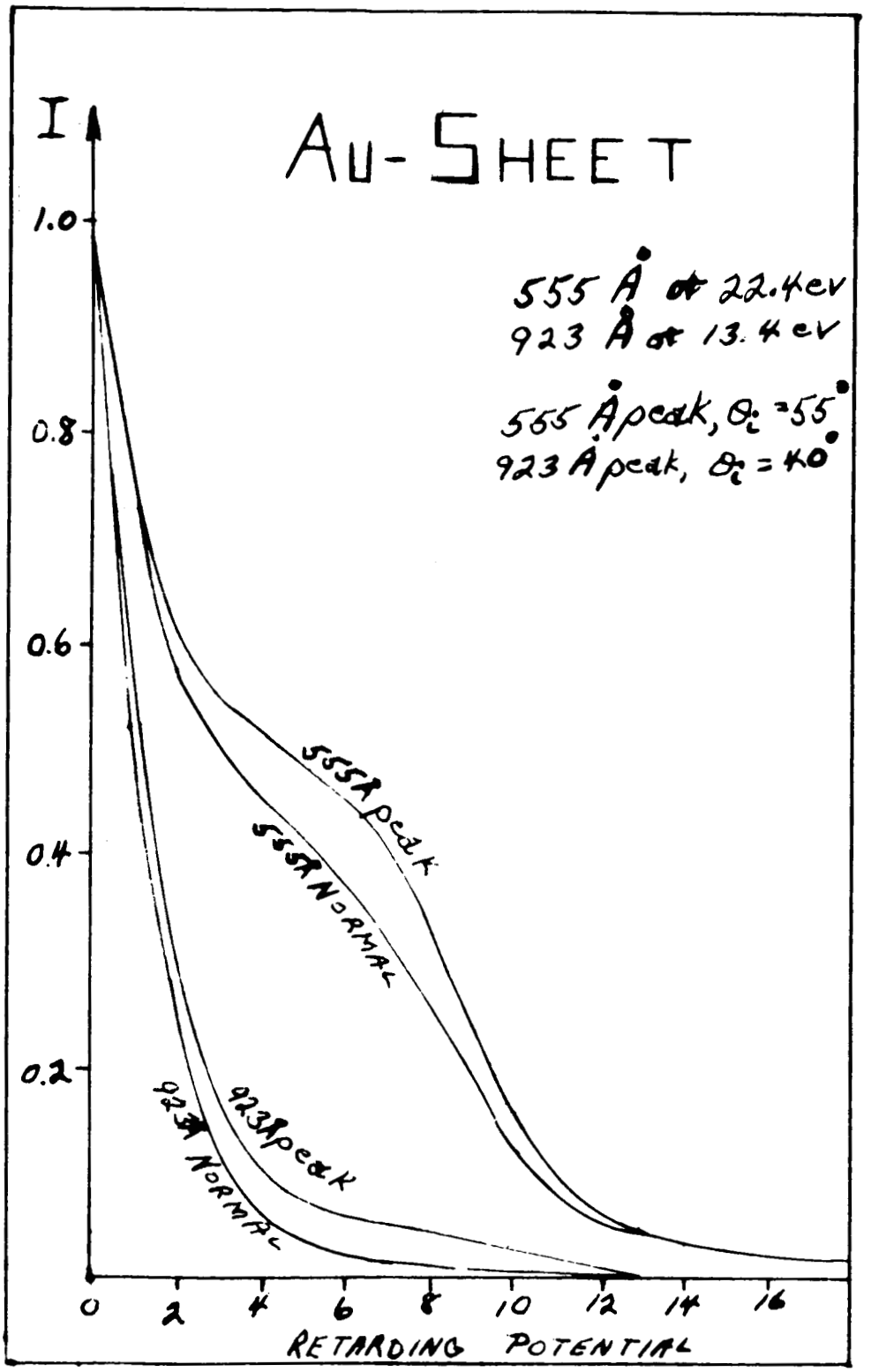

Fig. 12. Photoelectric current, I, of a 10 mil gold sheet as a function of retarding potential for normal incidence and for the angle of incidence giving peak photoelectric yield with no retardation (see Fig. 11).

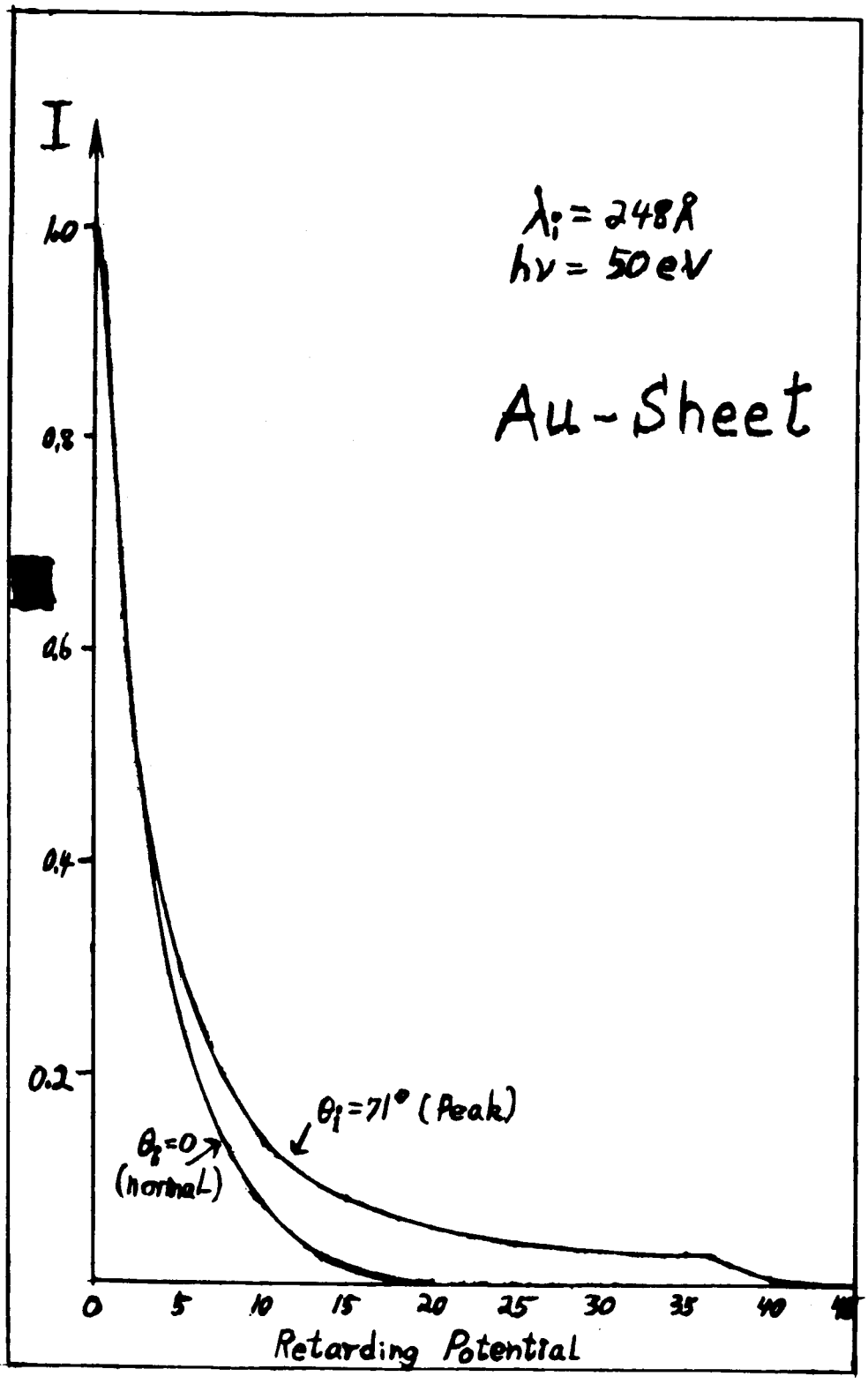

Fig. 13. Photoelectric current, I, of a 10 mil gold sheet as a function of retarding potential for normal incidence and for the angle of incidence giving a peak yield with no retardation (see Fig. 11).

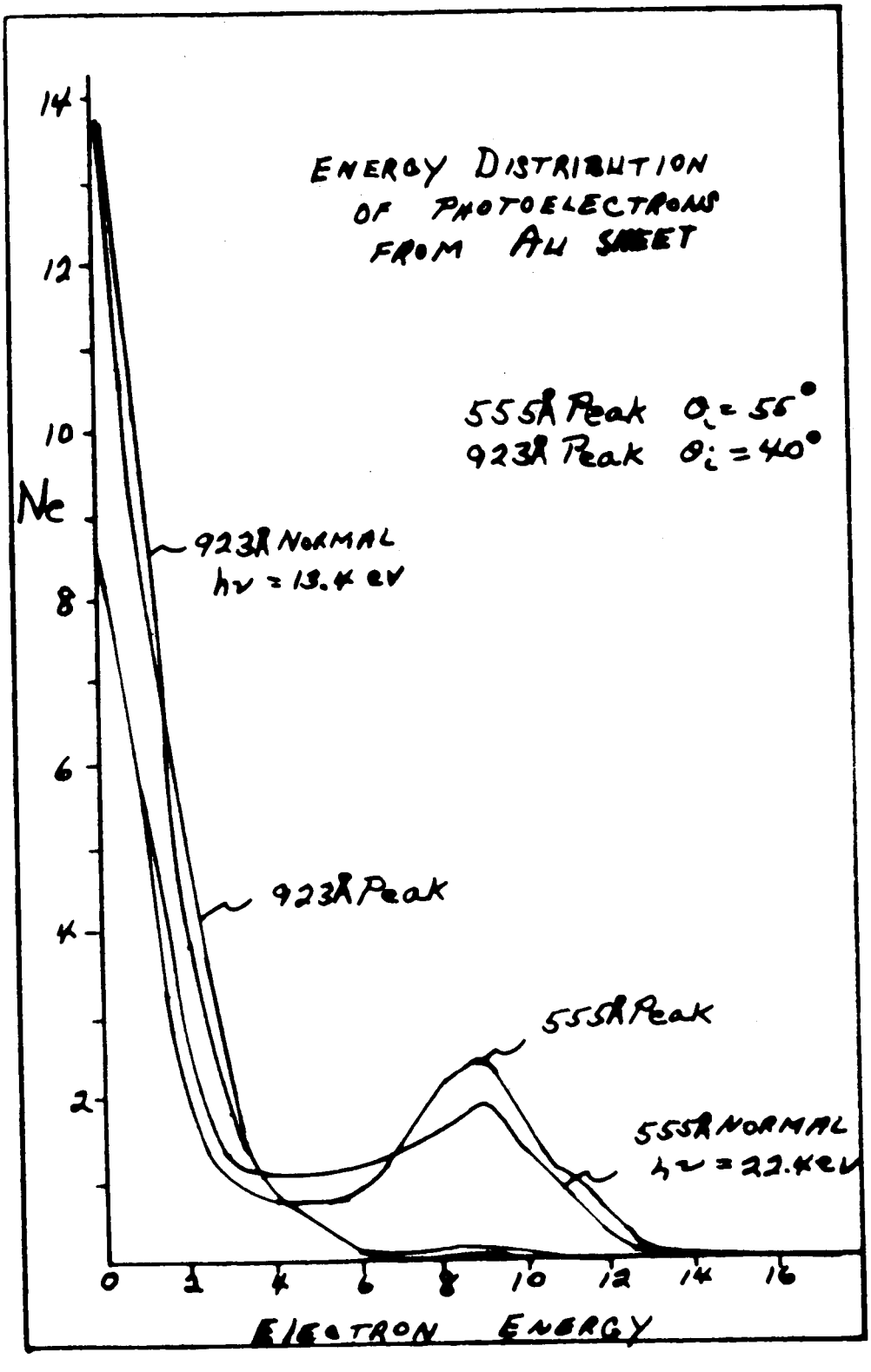

Fig. 14. Energy distribution of photoelectrons from a 10 mil gold sheet for normal incidence and for the angle of incidence giving peak photoelectric yield. The incident wavelengths were 555 Å and 923 Å.

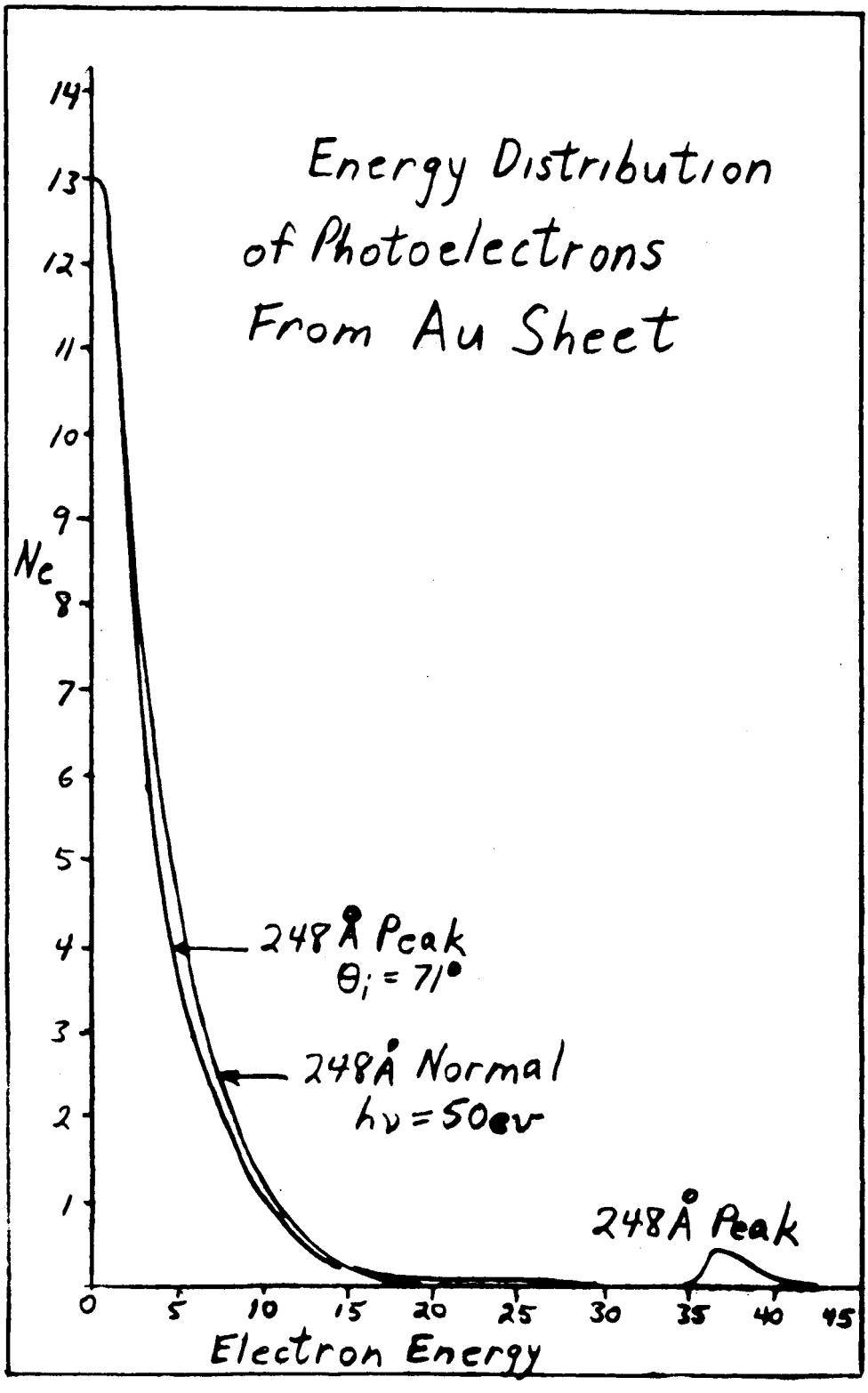

Fig. 15. Energy distribution of photoelectrons from a 10 mil gold sheet for normal incidence and for the angle of incidence giving a peak photoelectric yield. The incident wavelength was 248 Å.

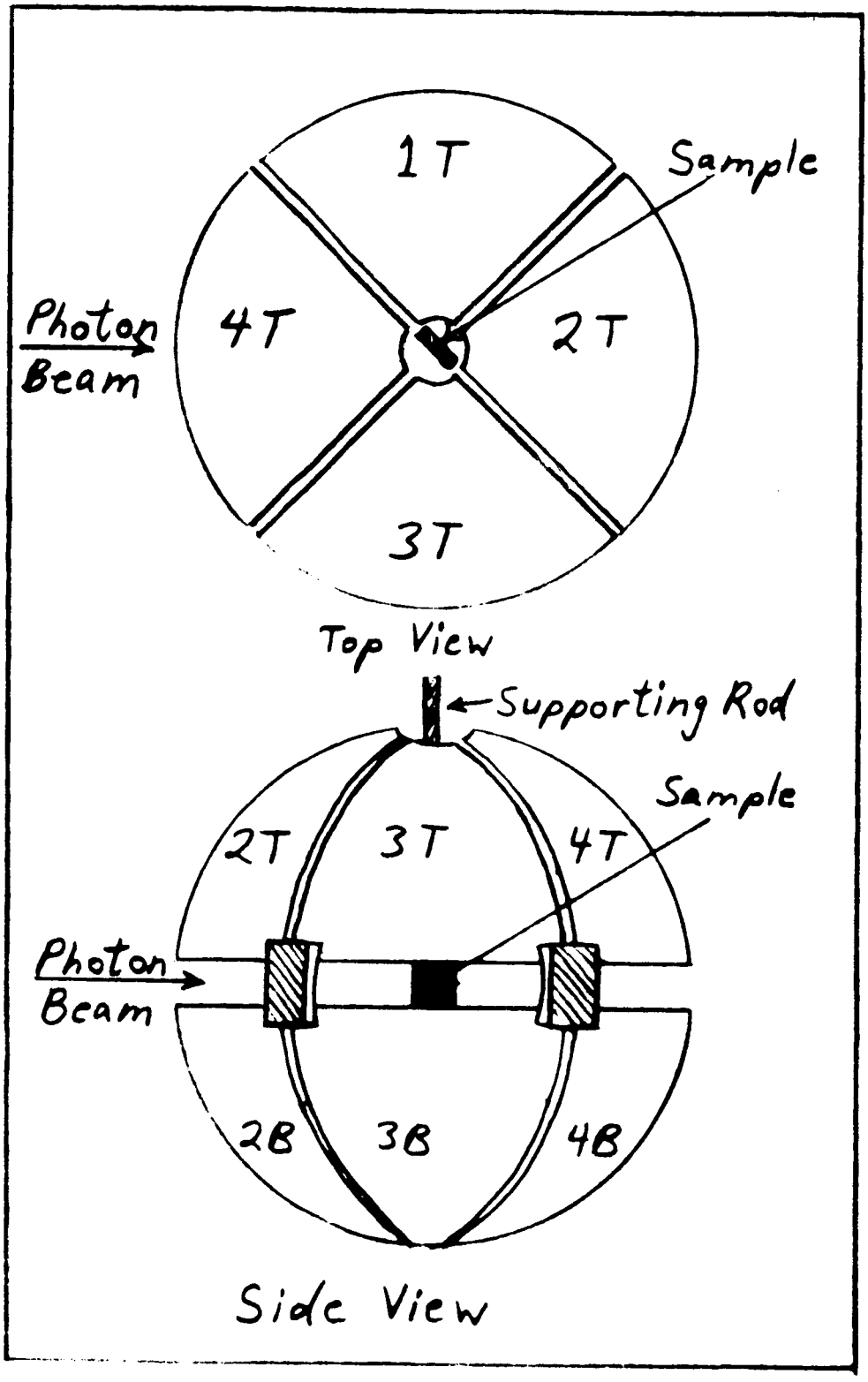

Fig. 16. Geometry of the spherical collecting system as it was used to take the data shown in Fig. 17. The sample position shown corresponds to an angle of incidence of 45° in Fig. 17.

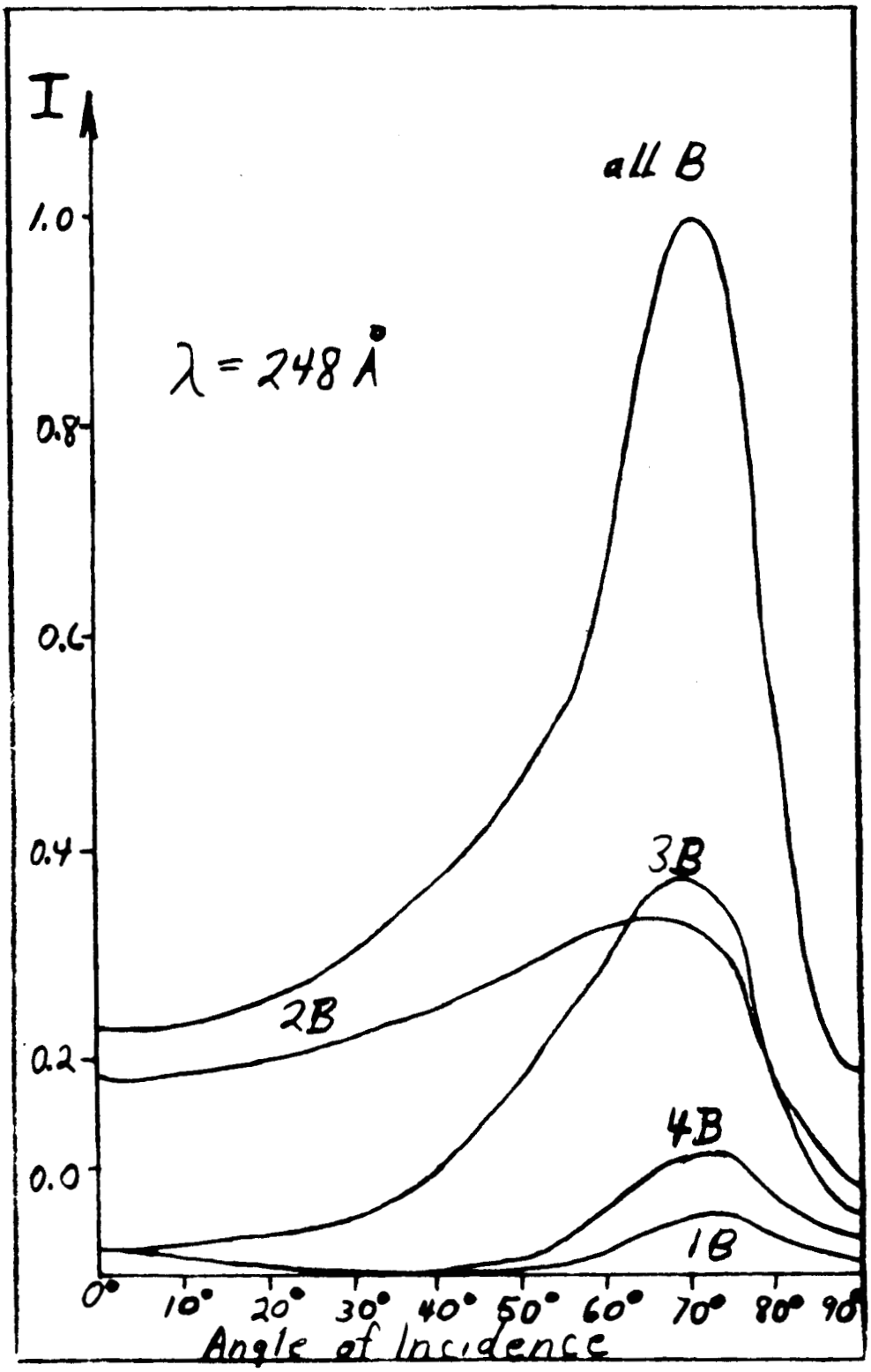

Fig. 17. Photoelectric current of a 10 mil gold sheet as a function of the angle of incidence. The top curve represents the current collected by the bottom hemisphere with the screen and top hemisphere grounded. The lower curves show the current collected by each of the four bottom octants as labelled, corresponding to the electrode geometry illustrated in Fig. 16.

before leaving the surface to become free. The present preliminary results indicate that perhaps very little such scattering occurs, and that therefore vectorial or polarization effects are highly significant. Thus, our work on thin films is likely to yield important new information with respect to the mean-free path of low energy electrons within the metal itself. In addition, the two humps in the photoelectron energy distribution curves may indicate the interaction of a photon of fixed energy with two electrons in different energy states. It is clear from the current results that much valuable work can be done with the existing apparatus.

It is planned to spend the period between the time of this writing and the time of our move into new quarters on the type of measurements mentioned above, specifically on transmitting thin aluminum films. Some of this work has been done earlier in this laboratory and reported recently in the literature.[6] In addition, the undersigned has also reported on the status of this research and the work planned for the immediate future in an invited paper at the recent "International Conference on the Physics of X-Ray Spectra," held at Cornell University, June 22 to 24, 1965.[7]

A number of thin films which have been found in this laboratory and others to show considerable transmission in the vacuum ultraviolet range will be used initially in this

---

[6] O. P. Rustgi and G. L. Weissler, J. Opt. Soc. Am. 55, 456 (1965).

[7] G. L. Weissler, Bull. Am. Phys. Soc., to be published (1965).

work. When the apparatus as shown in Fig. 9 is being moved to our new quarters after January 1966, it is planned to couple to the 18" experimental chamber, shown in Fig. 9, a Seya monochromator. The preparations for the Seya have been made and Fig. 9 indicates the place of attachment of the Seya. This combination of a Seya and Vodar monochromator to the same experimental chamber would thus allow a study of all the optical and photoelectric properties mentioned above over a very wide wavelength range, theoretically from 10,000 Å down to 100 Å. The period from January to June 1966 will be used to reassemble the apparatus with the combination of the Vodar and Seya both being attached to the 18" diameter experiment chamber.

25 copies respectfully submitted,

G. L. Weissler
Professor of Physics
Chief Investigator
NASA Grant No. NsG-178-61

15 October 1965